

# Wave Energy Resources Along the European Atlantic Coast

Philippe Gleizon, Francisco Campuzano, Pablo Carracedo,  
André Martinez, Jamie Goggins, Reduan Atan and Stephen Nash

## Introduction

Requirements for reducing industrial carbon dioxide emissions, together with the depletion of fossil fuel reserves and the need for more secure energy, drive governments and energy industries to diversify their energy sources and consider more sustainable resources. Renewable energy has become a credible alternative to fossil fuels for meeting the increasing energy demand of industrialised societies. Most renewable energy already produced is from hydraulic, wind, and solar power. In contrast, marine energy represents a tiny proportion of current energy production. Yet, the Atlantic Coast of Europe has one of the most important marine renewable energy resources in the world in terms of tidal range such as in the Severn Estuary (UK) or Saint-Michel Bay (France), tidal stream such as in the Pentland Firth (UK) or near Alderney Island (UK/France), and waves.

Conscious of Europe's abundant renewable energy resources, the European Commission has adopted a proactive attitude to encourage, promote, and develop

---

P. Gleizon (✉)

Environmental Research Institute, University of the Highlands and Islands,  
Thurso, UK  
e-mail: Philippe.Gleizon@uhi.ac.uk

F. Campuzano

Maretec, Instituto Superior Técnico, Universidade de Lisboa,  
Avenida Rovisco Pais, Lisbon, Portugal

P. Carracedo

Meteogalicia, San Lazaro S/N, Santiago de Compostela, Spain

A. Martinez

EIGSI, 26 rue Vaux de Foletier, La Rochelle, France

J. Goggins · R. Atan · S. Nash

College of Engineering and Informatics and Marine Renewable Energy  
Ireland Research Centre, National University of Ireland, Galway, Ireland

**Table 1** Targets of renewable energy source (RES) as a percentage of gross final consumption, and marine energy contribution (installed capacity and gross electricity generation) for the five Atlantic European countries in 2020 and 2015 (NREAP 2010)

	Target—2020			Target—2015		Installed—2014	
	% RES ( $S_{2020}$ )	Capacity (MW)	Energy (GWh)	Capacity (MW)	Energy (GWh)	Capacity (MW)	Energy (GWh)
France	23	380	1150	302	789	240	414
Ireland	16	500	1533	0	0	0	0
Portugal	31	250	437	60	75	1	0.026
Spain	20	100	220	0	0	0	0
UK	15	1300	3950	0	0	3	2

the production of energy from these resources. The European Union Renewable Energy Directive has set a binding target to all member states of providing 20% of energy supply with renewable energy by 2020 and at least 27% by 2030 (European Commission 2015). Each European country has proposed a National Renewable Energy Action Plan (NREAP 2010) submitted under the Article 4 of Renewable Energy Directive 2009/28/EC, setting their national targets for renewable energy in accordance with their national energy consumption rates and available resources and aligning them with the European targets. Note that the National Renewable Energy Action Plan (NREAP 2010) gives a comprehensive strategy but does not differentiate between the different types of marine energy, and they encompass other marine energy sources such as thermal or osmotic energy.

Table 1 summarises for each of the five Atlantic European countries the targets for the contribution of energy production from renewable sources as a percentage of gross final energy consumption ( $S_{2020}$ ), and the projected installed capacity and electricity generation of marine energy for 2015 and 2020. Although it has the lowest  $S_{2020}$ , the United Kingdom (UK) has the most ambitious targets for marine resource development of the five countries. It plans to increase its capacity by 1300 MW within 5 years. This target is considered achievable because of the abundance of the combined marine energy resources of tidal range, tidal stream, and waves. France already had some marine energy capacity because of the tidal power plant in La Rance estuary. The plant has been operating since 1967 and has a capacity of 240 MW. Portugal developed the first commercial wave site at Aguçadoura (near Porto), which unfortunately was short-lived because of a bearing problem on the first generation of Pelamis attenuators, and has been operating a pilot Oscillating Water Column plant on the Island of Pico (Azores) since 2006. The installed marine capacity in 2015 has not yet been reported, but progress towards targets can be estimated from the 2014 capacity reported to the European Commission (Table 1).

The current contribution of marine energy in the renewable energy scheme remains limited compared to other renewable sectors. Tidal energy is geographically constrained to few sites where available energy is sufficient to make the sites

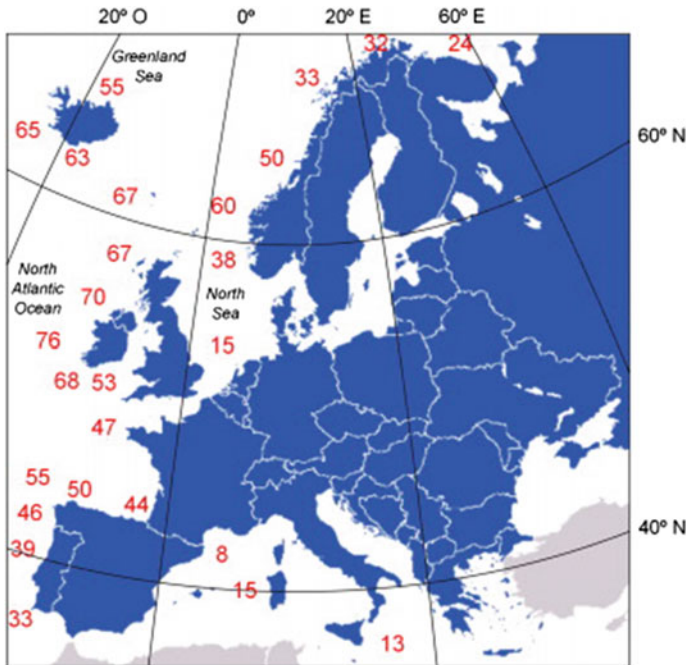


**Fig. 1** Estimated annual mean power distribution in Europe (Lopez et al. 2013)

profitable. Conversely, the wave resource is more widely distributed and is therefore a promising source of energy, but the distribution of wave activity depends largely on the fetch and is mainly concentrated between 30° and 70° north and south latitudes (Barstow et al. 2008, 2009). A bulk estimate of the annual wave power distribution in Europe shows that it can reach up to 76 kW/m off the western coast of Ireland (Fig. 1). However, the commercial development of this source of energy is likely to be one of the latest due to (1) its relatively recent technological development and therefore the relative lack of tried and tested engineering solutions and (2) the uncertainty of resource availability mainly because of the inherent unpredictability of long-term wind and therefore wave climate. Therefore, a thorough evaluation of the resources is essential to assessing the energy yield of a potential site.

The transnational project EnergyMare was commissioned to investigate the potential of marine renewable resources along the European Atlantic Coast, to test innovative monitoring techniques and to promote the development of test sites. Through a collaborative partnership, existing computing and monitoring resources have been combined to produce a comprehensive picture of the wave resources on the European Atlantic shelf that provides both a holistic description of the wave climate and detailed maps of sites of potential interest.

**Fig. 2** Atlantic Europe  
general view



The European coastline shows an irregular outline in the most exposed regions of western Scotland (UK), western Ireland, Bretagne (France), and Galicia (Spain) (Fig. 2). These regions are characterised by rocky shores and a succession of cliffs, rock outcrops, and sandy bays. These coastal features reveal the presence of high wave activity on a geology dominated by igneous or metamorphic rocks (May and Hansom 2003). In addition, there are more than 700 islands around Scotland, most of them distributed in three major archipelagos—the Shetlands, Orkneys, and Hebrides. The coast of Galicia is also irregular, featuring the presence of numerous headlands and rías (inlets), such as the Rías Baixas in the west. It is more open than the Scottish Coast and features longer stretches of sandy bays. Except in the Lisbon–Setubal area, the Portuguese coastline is more linear, but the bathymetry

**Fig. 3** Bathymetry offshore the Portuguese coast (Fig. 2 red inset)



reveals the presence of three sets of submarine canyons near the coast: Nazaré Canyon, Lisbon and Setúbal Canyons, and St. Vincente Canyon (Fig. 3). The bathymetry near the canyons deepens quickly from 50 m on the continental shelf to more than 300 m at the bottom of the canyon (e.g. Nazaré Canyon). Although they generally have very minor impacts on wind waves, under specific swell conditions, these canyons create conditions for occasional giant local waves (30 m) well known to surfers.

These coastal and bathymetric irregularities can influence the wave patterns near the coast and consequently introduce small-scale variability in wave energy distribution. Getting refined estimates at the areas of interest is therefore of prime interest for the wave industry, stakeholders, and regulators.

A description of wave resources can be obtained from long-term hindcasts of spectral wave models and can be supported by monitoring data. Third-generation spectral models have become the state of the art in wave modelling. Few of these models have emerged from the same fundamental equations and processes. The most common are the Wave Model (WAM), WaveWatch III, Simulating Waves Near-shore (SWAN) model, TELEMAC-based Operational Model Addressing Wave Action Computation (TOMAWAC), and MIKE21-SW. A more comprehensive description of these models is given in a previous chapter by Robertson (2016).

The first comprehensive description of wave energy resources in Europe was provided by the Wave Energy Resource Atlas (WERATLAS) project (Pontes 1998)

funded by the JOULE/THERMIE programme. The WAM was used to calculate the wave parameters, significant wave height  $H_s$ , mean wave energy period  $T_e$ , peak period  $T_p$ , mean direction  $\theta_m$ , and energy flux per unit crest length  $P_w$  over the European continental shelf (49°W–45°E; 26.5°N–73°N). The values were calculated based on 85 data points of which 41 were in the Atlantic Ocean. Data collection, analysis, and interpretation were performed over the period from 1987 to 1994 for the Atlantic Ocean. WERATLAS gave the first wave hindcast at a synoptic scale but on a coarse grid (Pontes 1998; Pontes et al. 1998). The planning and development of energy sites requires finer characterisation of the wave energy to optimise the cost/benefits by selecting the most appropriate devices and array layouts. In particular, a finer wave resource characterisation could be needed in the presence of irregular coastline or complex bathymetry, which can affect the wave characteristics over short distances.

To complete a fine-resolution assessment of the wave resources at a local scale, state-of-the-art wave models were applied on unstructured or high-resolution structured meshes (see Bertotti and Cavaleri 2012). Venugopal and Nemalidine (2015) set the spectral wave module MIKE21-SW of the MIKE21 modelling suite (DHI 2007) on an unstructured grid over the UK/Scotland waters, with fine-resolution characterisation down to 0.0005 square degrees in the Orkneys and Pentland Firth waters. The boundary conditions for this model were taken from predictions of a large-scale MIKE21-SW model extending over the North Atlantic Ocean and the North Sea (10°N–70°N and 75°W–10°E). The UK model was run for short periods during 2011 and 2012, and it was successfully validated against wave buoy data recorded at five locations around Scotland. The validation produced correlation coefficients that were higher than 0.96, for the significant wave height. The spatial distribution of the mean significant wave height and wave power around Scotland was found to be consistent with the atlas of UK renewable energy (ABP MER 2008), but with a much higher resolution, because the maps from the atlas are based on a 12 km model grid resolution in coastal areas. The wave power distribution was lowest on the eastern coasts of Scotland and highest on the western coasts, where the mean was estimated to be between 40 to 45 kW/m and the maximum values were estimated to be up to 650 kW/m near the Hebrides and Shetlands shores during January–December 2010.

Guillou and Chapalain (2015) implemented the nearshore spectral wave model SWAN on an unstructured mesh over the Sea of Iroise, in western Brittany, France, with the cell edges varying from 10 km offshore to less than 300 m nearshore. The wave power was averaged over a 7-year (2004–2011) hindcast modelling period. This regional wave model was driven by three-hour time interval wind data at a spatial resolution of 10 km obtained from Météo-France's meteorological model ALADIN, and wave components (significant wave height, peak period, peak direction, and spreading) predicted by a regional run of the large-scale spectral wave model WaveWatch III with a spatial resolution of 18 km and a temporal resolution of 3 h. The validation of the model predictions against nine wave buoy measurements gave values of Pearson correlation coefficient between 0.88 and 0.98 for the significant wave height and between 0.5 and 0.78 for the peak period.

**Fig. 4** Brittany (Fig. 2 *white inset*)



The annual mean wave power near the coast showed a strong variability around 20 kW/m, influenced by the shadowing effect of the Ushant Archipelago in the north and Sein Island in the south (see Fig. 4). Seasonal variations show a marked difference between the summer months when wave activity is consistently low, and winter months when wave activity is high on average but less consistent from one year to another. In a parallel study, Guillou (2015) investigated the difference between the third-generation spectral wave models SWAN and TOMAWAC, using the same grid, input data, period of simulation, and the most accurate parameterisation for both models. The comparison between these two models revealed that SWAN gives lower estimates of mean wave power in offshore waters than TOMAWAC but similar estimates in onshore waters. The comparable results for the significant wave height in offshore waters suggest that the main difference could be due to the computational methods used for wave period or the energy propagation.

Iglesias et al. (2009) investigated the wave energy potential in Galicia using the nearshore spectral wave model SWAN (Booij et al. 1999) on a  $200 \times 200$  m grid. The open boundary conditions were provided by a large-scale WAM ( $18^{\circ}\text{N}$ – $69^{\circ}\text{N}$  and  $60^{\circ}\text{W}$ – $9^{\circ}\text{W}$ ) with a coarser resolution of  $0.25^{\circ}$  (approx. 30 km). The model was run over the period from 1996 to 2005 to derive a hindcast for the wave climate and wave power at various sections of the Galician coast (for locations, see Figs. 2, 13, and 15g)—Costa de la Muerte (Iglesias and Carballo 2009), Cape San Adrian to Cape Ortega (Iglesias et al. 2009), and Estaca de Bares area (Iglesias and Carballo 2010c). The model was extended to the north coast of Spain to the Asturias coastal region (Iglesias and Carballo 2010a) and the Bay of Biscay (Iglesias and Carballo 2010b). These fine-scale models applied near an irregular coastline and in the presence of a highly variable bathymetry showed that the wave energy potential can be doubled or halved over distances of only few kilometres, due to refraction, shoaling, bottom friction, sheltering, and diffraction from islands and headlands.

These studies emphasise the variety of spectral wave models and their range of applications. Although all of these third-generation spectral models use the same fundamental formulation to represent wave propagation—here the spectral action balance equation—they may differ in their numerical techniques or their

representation of source–sink terms, for instance, for the wind input, whitecapping, or nonlinear wave–wave interactions (WISE Group 2007).

The existing wave models, developed by the EnergyMare project partners, used primarily WaveWatch III and SWAN, which were combined to provide a holistic view and a detailed description of the wave resources along the Atlantic Coast. In the next section, the commonalities and differences of the relevant spectral wave models are presented, with an emphasis on WaveWatch III and SWAN. This introduces a more specific description of each model and its validation against monitoring data when applicable. In the last section, the spatial distribution and temporal variability of wave energy resources across areas of the European Atlantic coastal waters, based on medium-/long-term hindcast, are presented in term of resource availability and risk to installations.

## Spectral Wave Modelling

### *Overview of Models*

The third-generation spectral wave models, developed in the late 1980s, allow for free development of the wave spectrum without any specific shape constraint. In particular, they include the energy transfer between resonant frequencies from quadruplet wave–wave nonlinear interactions (Haselmann 1962).

The so-called progressive wave models, such as WAM (WAMDI Group 1988) or WaveWatch III (Tollman 1990), are suitable for modelling wind waves in deep seas; they proved to be less accurate in coastal waters for reasons that are presented later. The SWAN model was specifically designed based on the initial WAM source code to improve wave prediction capability nearshore (Booij et al. 1999), but it is less suitable for modelling waves in the open ocean. From this point of view, estimating the wave energy resource both on synoptic and local scales can be challenging and may require a combination of the different models.

### WAM

The first spectral wave model WAM was developed by the so-called WAMDI Group (WAMDI Group 1988) and is still operated by the European Centre for Medium-Range Weather Forecasts (ECMWF), which provides wave hindcast data over the global ocean and on nested domains such as the North Atlantic Ocean. The action density balance Eq. (1) is solved by a two-time level fully implicit integration scheme (Hersbach and Janssen 1999):

$$\frac{\partial N}{\partial t} + \vec{\nabla}_{\vec{x}} \cdot \left( \left( \vec{c}_g + \vec{U} \right) \cdot N \right) + \frac{\partial c_\sigma N}{\partial \sigma} + \frac{\partial c_\theta N}{\partial \theta} = \frac{S_{tot}}{\sigma} \quad (1)$$

where  $N(\vec{x}, t; \sigma, \theta)$  is the action density defined from the energy density  $E(\vec{x}, t; \sigma, \theta)$  by  $N = \frac{E}{\sigma}$  and depends on space  $\vec{x}$ , time  $t$ , frequency  $\sigma$ , and direction  $\theta$ ;  $\vec{c}_g$  is the group velocity in the physical space;  $\vec{U}$  represents a current velocity;  $c_\sigma$  and  $c_\theta$  are the wave propagation velocity components in the spectral space, for frequency and direction, respectively; and  $S_{tot}$  encompasses all of the source/sink terms.

Besides the quadruplet wave–wave nonlinear transfer, the source/sink terms include whitecapping, bottom friction, duration, and fetch-limited growth from wind friction, which also takes into account the effect of wind gustiness and air density. Wave generation includes both linear (Cavaleri and Malanotte-Rizzoli 1981) and exponential growth (Komen et al. 1984) caused by wind stress. The model is operated on regular meshgrid. The WAM model proved to be reliable for deep water and therefore the open ocean, but the absence of shallow-water processes, such as depth-induced breaking or triad nonlinear wave interactions (Booij et al. 1999), made the model less accurate nearshore, in spite of late implementation of a depth-controlled algorithm for maximum wave energy and frequency down shifting. The impact of currents on waves is often minimal except in shallow nearshore areas, in particular inside the entrance of bays and harbours where tidal currents can be strong (Yang and Wang 2015).

### WaveWatch III

Soon after WAM became operational, the National Oceanic and Atmospheric Administration (NOAA) developed the spectral wave model WaveWatch III to account for wave–current interactions in unsteady conditions (Tolman 1990). The main difference between the WAM and the WaveWatch III model is their numerical technique. Due to their complexity, the numerical schemes used by WaveWatch III cannot be detailed but, in summary, it calculates the solution of the action density balance Eq. (1) using a time-splitting approach. Four different time steps are used:

- a global time step in which the entire solution is propagated, which includes winds and currents;
- a time step for spatial propagation; this time step is adjusted on the wave frequencies to ensure numerical stability and optimise the computing time;
- a time step for the intra-spectral propagation; and
- a time step to integrate the source terms, giving more accurate calculations for rapidly changing wind and wave conditions.

The default numerical scheme for wave propagation in WaveWatch III is the ULTIMATE QUICKEST scheme (Leonard 1979, 1991) implemented both for the physical space and for the directional space ( $\theta$ -space). In the frequency space

( $\sigma$ -space), the scheme is adapted to take into account variable grid spacing, and a first-order upwind scheme is used for the lowest and highest wave numbers. These numerical techniques result in a more accurate replication of peak values and give a better representation of rapidly changing wind and wave conditions. Until recently, WaveWatch III could only be implemented on rectangular grids, but the newest version 4.18 can be set up on an unstructured grid (Roland 2009).

## SWAN

The spectral wave model SWAN was developed from WAM to improve the accuracy of spectral wave modelling in the nearshore zone. Therefore, it uses the same scientific background and equations, but includes additional functionality such as triad wave-wave nonlinear interactions and depth-induced wave breaking (Booij et al. 1999). Recently, SWAN has also been designed to run on unstructured grids, which provide a more suitable resolution nearshore especially in the presence of irregular coastlines (Zijlema 2010).

The option of implementing SWAN on either structured or unstructured meshgrid has been a major improvement to the model. Unstructured meshgrids were essentially used in finite element models such as TOMAWAC (Robertson 2016). Tuomi et al. (2014) tested the response of a spectral wave model (WAM) on a structured grid over an archipelago in the Gulf of Bothnia (Baltic Sea). They demonstrated that the model overestimated the wave energy propagating through the archipelago mainly because of slight inaccuracies in the representation of refraction and dissipation effects. The predictions are improved by using finer grids but at considerable expense of computing time. Unstructured grids allow for fine-resolution mapping nearshore and a better representation of convoluted coastlines, resulting in improved predictions as shown in the wave resource assessments of Robertson et al. (2014, 2016) conducted on the western coast of Vancouver Island, Canada. Implicit schemes are generally used with unstructured grid to avoid stability restrictions imposed by the Courant-Friedrichs-Lewy criterion. For the equation discretisation, SWAN uses an implicit Euler scheme solved by a three-direction sweep Gauss-Seidel relaxation technique to ensure a convergence of the solution for all grid points (Zijlema 2010). To avoid instability problems, the model does not allow triangular elements that have an angle wider than  $143^\circ$ .

Different numerical schemes are used for discretising the equations, depending on the type of simulation, node location, and user choice. First, a fully implicit first-order upwind scheme, which is robust and unconditionally stable but introduces numerical diffusion, was implemented (Booij et al. 1999). This scheme provided an accurate enough solution for wave propagation in the geographical space, but the spectral space required higher accuracy. More advanced schemes were introduced to improve the accuracy. For instance, nonstationary computations use the Stelling and Leendertse scheme (Stelling and Leendertse 1992), except next to boundary nodes where the first-order upwind scheme applies. The Stelling and

Leendertse scheme is known to have such a small numerical diffusion that it can generate a so-called garden sprinkler effect due to spectral resolution over large grid intervals. To counteract that effect without increasing the numerical diffusion too much, a diffusion tensor can be added to the propagation equation (Booij and Holthuijsen 1987; Tolman 2002). In a more recent development, limiters were introduced to reduce local errors due to excessive transfer of energy in the spectral propagation by refraction or frequency shifting where the bathymetry representation is too coarse (Dietrich et al. 2013).

## ***Model Set-up and Validation***

To obtain wave statistics along the European Atlantic Coast, wave hindcast modelling was carried out using WaveWatch III and SWAN over five distinct coastal zones: Scotland (UK), Ireland, France, Galicia (Spain), and Portugal.

### **Scotland**

The irregular coastline of Scotland and the presence of archipelagos required that the model be run over an unstructured grid to provide good nearshore resolution without affecting computing time too much and to represent more accurately the attenuation of wave energy through the archipelagos (Tuomi et al. 2014). The hindcast was therefore performed by running SWAN on an unstructured mesh extending from  $10^{\circ}$  to  $0^{\circ}$ W and from  $56^{\circ}$  to  $62^{\circ}$ N (Fig. 5). The grid has

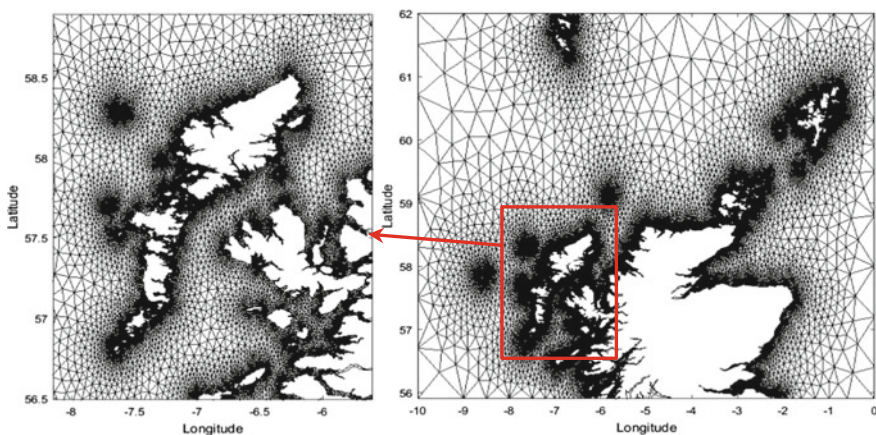


**Fig. 5** Meshgrid for the Scotland wave model for the entire domain (*right*) and a detailed view of the Hebrides Islands (*left*)

approximately 48,000 nodes and more than 83,000 elements with a minimum edge of  $\sim 50$  m. The model was run with a time interval of 3 h over a 10-year period (2004–2014).

The bathymetry was obtained from three different sources and at three different resolutions:

- SeaZone—1 arc second, for coastal areas and around archipelagos where the grid has the finest resolution;
- SeaZone—30 arc seconds, for nearshore areas covering most of the Scottish shelf; and
- GEBCO (General Bathymetric Chart of the Oceans)—1 arc minute, for the remaining offshore areas mainly near the northern, north-western, and eastern boundaries where the grid is coarser.

The bathymetry data were then averaged over the Voronoï cells related to the grid and integrated with the model.

Wind forcing uses 10 m elevation wind obtained from ECMWF reanalysis data on a  $0.75^\circ$  grid interval and 3-hour time interval. Sensitivity tests performed using the National Aeronautics and Space Administration's Modern Era Retrospective-analysis for Research and Applications (MERRA) reanalysis wind data at the same elevation but with finer spatial ( $0.5^\circ$ ) and temporal (1-hour) resolution did not show much difference in the model results. However, the use of this fine-resolution data significantly increased the computational time, so the simulations were carried out using wind forcing from ECMWF wind data.

As presented by Gleizon and Woolf (2013) and Gleizon and Murray (2014), swells can travel long distances and influence wave energy even in the centre of the domain of a model of that scale. Wave boundary conditions were obtained from the predictions of a large-scale model (WaveWatch III) covering the North Atlantic basin and were specified as two-dimensional energy density spectra.

In addition to wave generation by wind forcing, the parameterisation of the model included other source/sink processes: triad and quadruplet wave–wave nonlinear interaction; bottom friction using a JONSWAP (Joint North Sea Wave Project) formulation with a constant friction coefficient of  $0.038 \text{ m}^2 \text{ s}^{-3}$ , which can be applied both for wind waves and for swell conditions (Hasselmann et al. 1973); whitecapping using a nonlinear saturation-based formulation (Van der Westhuysen et al. 2007); and wave breaking. However, sensitivity tests showed that these effects are minor compared to the generation by wind forcing and the boundary conditions.

The development of the model was supported by extensive wave monitoring data in the early 2010s. The locations, monitoring periods, and responsible institutions for the control of the wave buoys are listed in Table 2 and depicted in Fig. 6. The moored buoy K7, maintained by the UK Met Office, has been the longest operating buoy in the area and is part of a national meteorological surveillance network.

More accessible are the historical data from the Centre for Environment, Fisheries and Aquaculture Science (CEFAS) WaveNet directional waverider buoys. WaveNet is a strategic wave monitoring network for the UK. North of Scotland,

**Table 2** Wave monitoring period and location

Source	Location	Period	Long.	Lat.
ERI	Brim Ness	02/13–08/13	3.75°W	58.63°N
	Dunnet Bay	12/12–08/13	3.44°W	58.64°N
	Pentland F	01/12–07/12	3.28°W	58.68°N
	Wick	01/12–07/12	2.79°W	58.46°N
LCC	Bragar	10/11–09/12	6.91°W	58.43°N
	Siadar	10/11–09/12	6.72°W	58.50°N
CEFAS (WaveNet)	South Uist	02/09–05/12	7.91°W	57.29°N
	Moray F.	08/08–09/12	3.33°W	57.97°N
	Dounreay	10/97–05/01	3.75°W	58.59°N
Met Office	K7 buoy	04/92–11/01	4.50°W	60.70°N

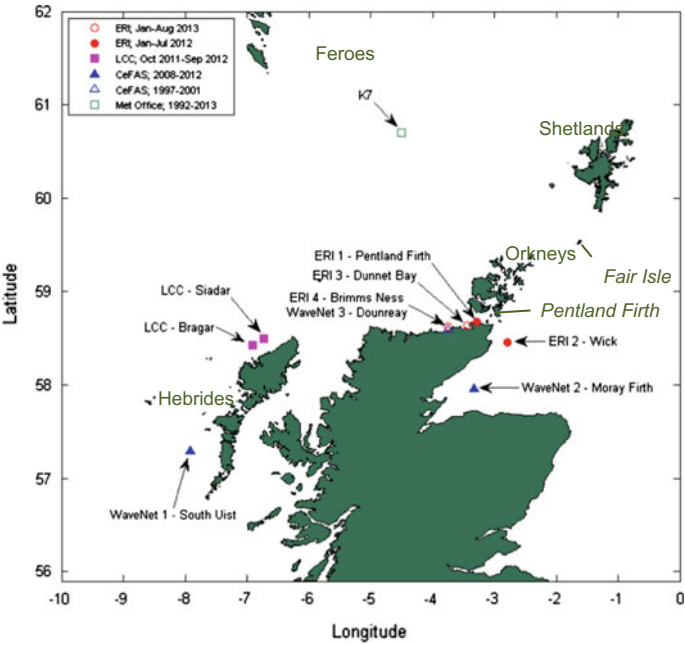


**Fig. 6** Wave buoy locations

only three buoys were deployed from the late 1990s up to today; they are in the West Hebrides (WMO ID: 62048; referred here as South Uist), Moray Firth (WMO ID: 62046), and Dounreay (decommissioned in 2001).

Complementary wave data were provided by Lews Castle College (LCC)<sup>1</sup> who deployed directional Datawell waverider buoys MKIII off the north-east of Lewis

<sup>1</sup>University of the Highlands and Islands.

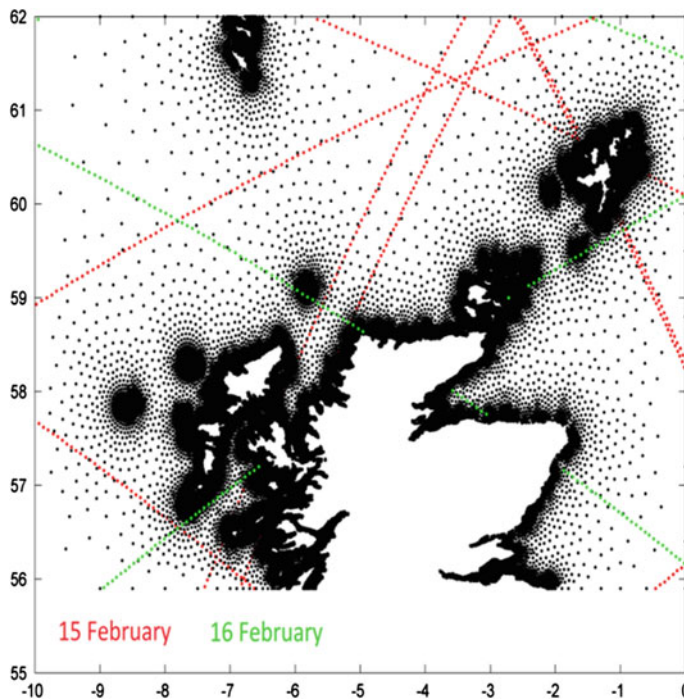


**Fig. 7** Satellite altimeter passes on 15 and 16 February 2011. The black dots indicate the model grid nodes

Island (Outer Hebrides) in 2011/12 at Bragar and Siadar. The records gave a range of statistical and spectral data.

Finally, the Environmental Research Institute (ERI)<sup>2</sup> deployed directional buoys MKIII for 6-month periods in 2012/13 at four different locations along the northern coast of Scotland: Brim Ness, Dunnet Bay, Pentland Firth, and Wick.

In addition to wave buoys, wave data were obtained from the CERSAT (Centre d'Expertise et de Recherche Satellitaire) database of the IFREMER (Institut Français de Recherche pour l'Exploitation de la Mer). The CERSAT database provides processed altimetry data collected from operational altimeter satellites (Piollé and Croizé-Fillon 2012). For the purpose of model validation, altimetry data for 15–16 February 2011 were downloaded from the database. These data, recorded by four altimeter satellites (ERS2, ENVISAT-GDR, Jason-1, Jason-2) during 11 passes during that period, give good coverage of the model domain (Fig. 7) that is complementary to the wave buoy data, in particular for offshore locations.

The model predictions are in a good agreement with monitoring data, as revealed by the coefficient of determination  $R^2$  values, which are between 0.81 and 0.91 for

<sup>2</sup>University of the Highlands and Islands.

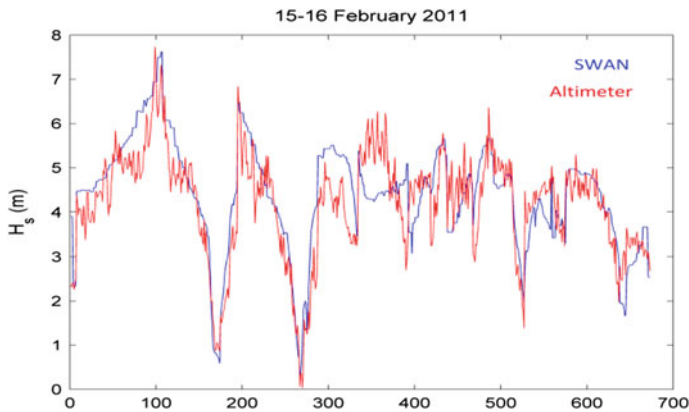


**Fig. 8** Comparison of predicted significant wave height with altimetry data on 15–16 February 2011

the significant wave height and between 0.6 and 0.79 for the mean period (Gleizon and Murray 2014).

The validation against altimetry data is more complex because the relevant model results must be extracted to coincide with time and space with the satellite passes. It was nonetheless possible to get a comparison with 681 points during two days of satellite passes (15–16 February 2011) that shows a good replication of observed significant wave height (Fig. 8).

## Ireland

The SWAN model was implemented on a regular grid with a grid interval of  $0.05^\circ$  ( $\sim 5.5$  km in latitude and  $\sim 3.3$  km longitude). The domain covers a large area around Ireland and over the Atlantic Ocean from  $20^\circ\text{E}$  to  $3^\circ\text{E}$ , and  $50^\circ\text{N}$  to  $59^\circ\text{N}$  (Fig. 9). The bathymetry with a resolution of 1 arc minute was obtained from the NOAA Centers for Environmental Information. The wind forcing was provided by ECMWF Era-Interim data with a spatial resolution of 0.5 degrees and a time interval of 6 h. The wave boundary conditions were obtained from global Wave-Watch III model data at 6-hour time interval, provided by the Fleet Numerical Meteorology and Oceanography Center. The model was run with a time interval of 1 h over a 7-year period (2008–2014).

Model calibration process involved a substantial number of sensitivity tests on model parameters, such as wind input, wave growth formulations, whitecapping, and bottom friction coefficients. The modelled output was compared to available data collected from four wave buoys off the Irish western coast (Fig. 9). The model calibrations show good correlation with monitoring data; the coefficient of determination  $R^2$  value is 0.9 for the significant wave height  $H_s$  and the  $R^2$  value is 0.8 for the mean period  $T_z$  at almost all four sites (Atan et al. 2015).

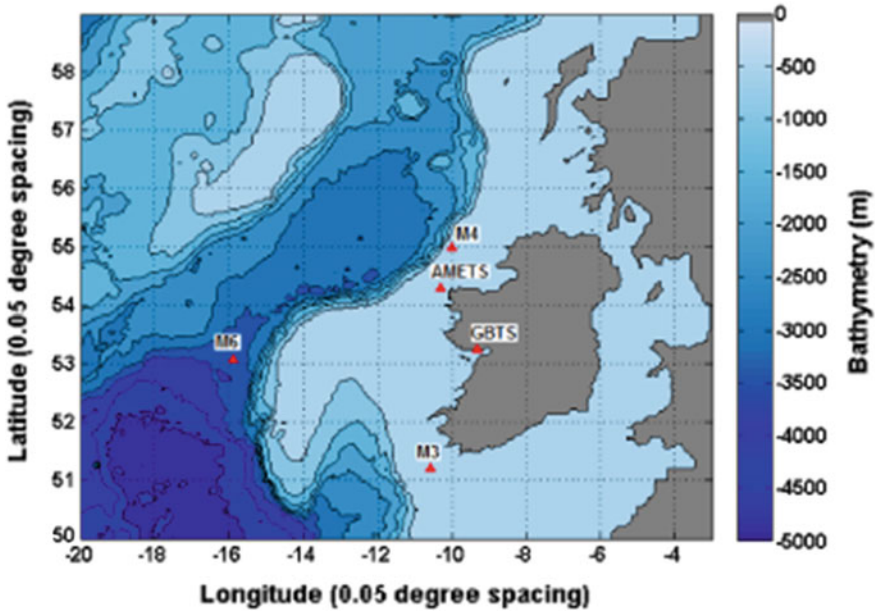


Fig. 9 Irish model domain and wave buoy locations

## France

The wave hindcast along the French coast was imported from the Previmer database. The hindcast was initially carried out by WaveWatch III over nine fine-resolution (200 m) regular grids covering the French coast from Dover Strait to the Bay of Biscay with a time interval of 1 h (Fig. 10). These grids were nested in a larger model domain extending from 10°W to 12°E and from 43°N to 58°N with a coarser grid resolution (4 km) and time interval (3 h). Wave hindcasts were obtained for a 7-year period, from 2008 to 2014.

The validation of the model predictions was done on a routine basis using data from Météo-France, CEREMA (Centre D'Étude et D'Expertise sur les Risques, L'Environnement, la Mobilité et l'Aménagement), ports and harbours for coastal validation, and IFREMER altimetry data for offshore validation. The models are also used to provide near-real-time forecasts of sea state.

## Galicia

The spectral wave model SWAN was applied on a high-resolution unstructured grid along the Galician coast to provide near-real-time wave forecast. The modelling domain extends up to 40 km offshore. The grid has a resolution from 100 m near the

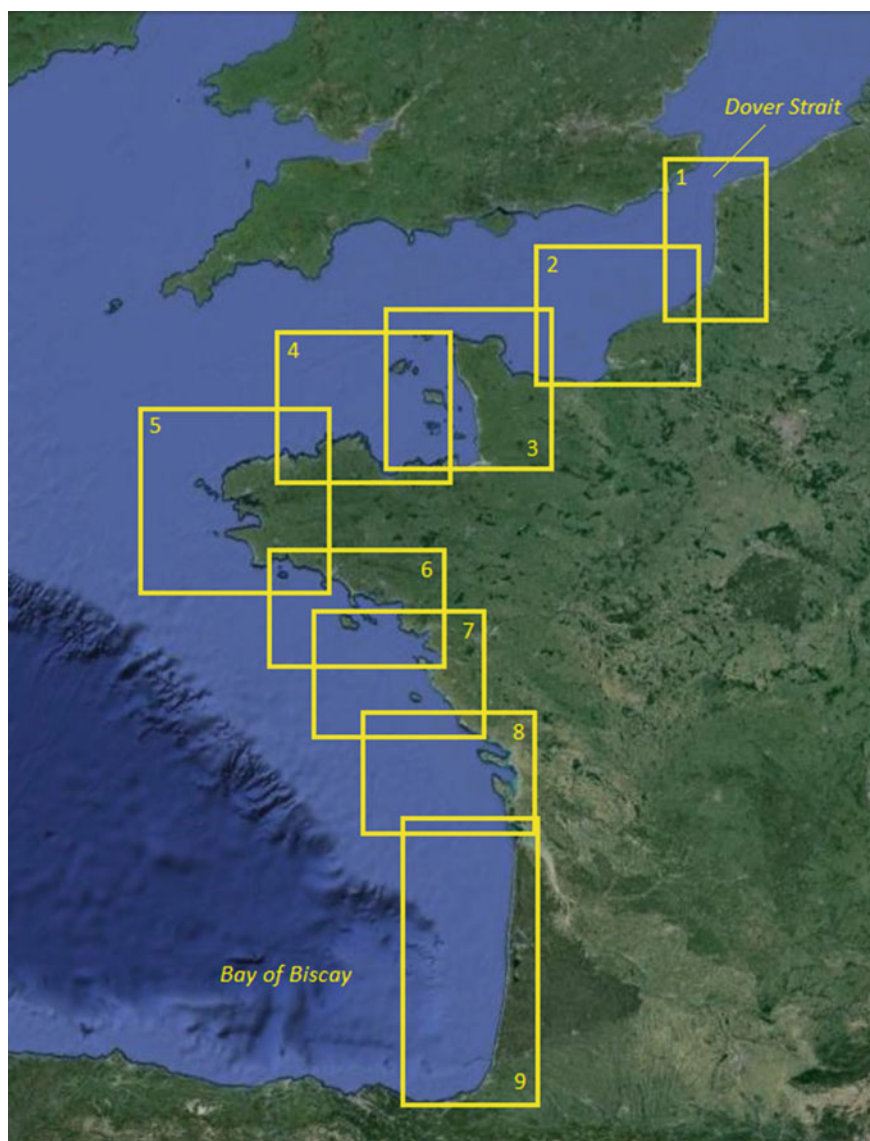


**Fig. 10** Sub-domains of the wave hindcast along the French Atlantic Coast

coast up to 8 km offshore (Fig. 11). The bathymetry was obtained from digitalisation of nautical charts made by Meteogalicia and InTeCMar (Institutotecnológico para o Control do Mediomariño). These data were filtered and interpolated to the unstructured mesh to provide the model with a high-resolution bathymetry.

The model provided a 42-year period wave hindcast, from 1958 to 2000. This extended period allowed for determining wave height for different return periods

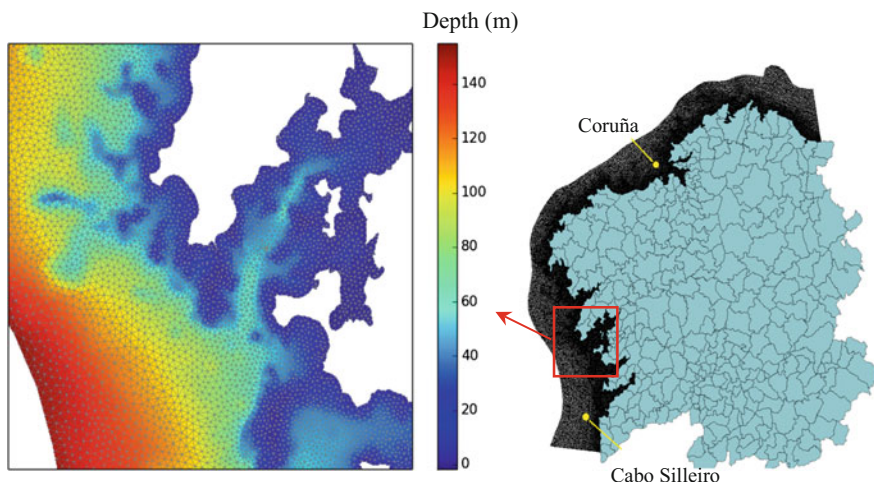


**Fig. 11** Meshgrid of Galician model for the entire domain (*right*) and a detailed view of the Rias Baixas area (*right*)

(2, 10, 25, 50, and 100 years), which can be used, for instance, for evaluating the risk to installations.

Because the model only covers a narrow band along the coast, it is primarily driven by the boundary conditions. Wave boundary conditions were obtained from a 6-hour interval hindcast from the HIPOCAS (Hindcast of Dynamic Processes of the Ocean and Coastal Areas of Europe) project (Guedes Soares et al. 2002). The model was validated against wave buoy data recorded by Puertos del Estado during February 2013 at two locations: Cabo Silleiro and Coruña (see Fig. 11). It showed close predictions of the model with the data, for both significant wave height and peak period (Gleizon et al. 2015).

## Portugal

The NOAA WaveWatch III v3.14 model was used to assess wave energy along the Portuguese coast. The model was applied on three nested grids (Fig. 12):

- a large-scale domain covering the North Atlantic Ocean (NAT) with a grid resolution of 0.5 degree;
- a continental-scale domain covering the south-west part of Europe (SWE) and extending from 23°W to 0°W and 33°N to 48°N with a grid resolution of 0.25 degree; and
- a coastal domain covering the Portuguese continental coast (PCC) and extending from 11.8°W to 7.4°W and 35.6°N to 42.8°N with a grid resolution of 0.05 degree.

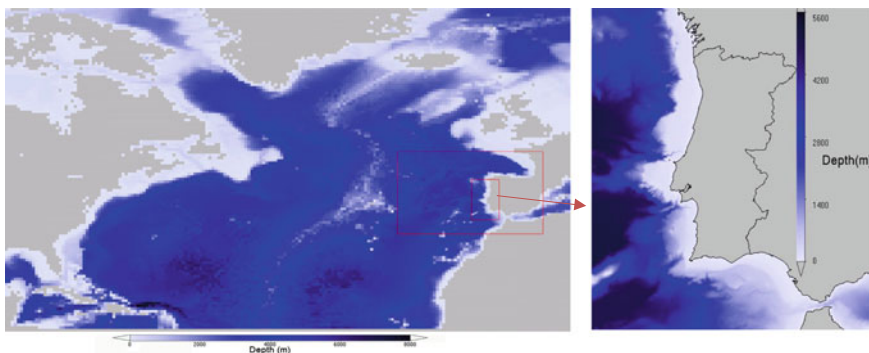


**Fig. 12** Domains of the WaveWatch III models for the Portuguese coastal application. Nested models are indicated by the *red boxes*

Different sources of bathymetric data were combined to populate the various nested models with appropriate resolution. The EMODNet (European Marine Observation and Data Network<sup>3</sup>) hydrographic portal provided fine-resolution bathymetry of 7.5 arc seconds, in particular for the nested models, and was completed by 30-arc second resolution global bathymetry data SRTM30\_PLUS (Becker et al. 2009) without EMODNet data.

The wave energy resource was evaluated using a hindcast covering the period from 2000 to 2010. The National Centers for Environmental Prediction (NCEP) FNL Operational Model Global Tropospheric Analyses (NCEP/NWS/NOAA/U.S. Department of Commerce 2000) was used to feed the wave models with wind intensities and directions from July 1999 on a time interval of 6 h and over a grid resolution of 1 degree. The wave boundary conditions for the SWE and PCC models were simply given by the larger scale models, NAt and SWE, respectively.

The SWE and PCC model hindcasts were validated against eight wave buoy stations distributed along the western coast of the Iberian Peninsula. The location of the wave buoys and validation results for significant wave heights and mean periods are summarised in Fig. 13 and Table 3.

The coefficients of determination  $R^2$  show a good correlation between predicted and measured values for the significant wave height ( $H_s$ ); values fell between 0.89 and 0.92, except near the southern coast at the stations of Faro and Cadiz where they have lower values around 0.8. The mean period generally shows less good correlation—the  $R^2$  values fell between 0.61 and 0.75 at most locations and were 0.2 and 0.31 at the southernmost stations of Faro and Cadiz, respectively. However, considering that areas of interest for the wave energy resources are mainly from the central to northern part of Portugal, the model was deemed sufficiently accurate for estimating the resource along this coast.

<sup>3</sup>[\[http://www.emodnet-hydrography.eu\]](http://www.emodnet-hydrography.eu).

**Fig. 13** Wave monitoring stations on the western Iberian Peninsula



**Table 3** Monitoring stations along the western Iberian Peninsula coast and coefficients of determination  $R^2$  for the significant wave height ( $H_s$ ) and mean wave periods ( $T_m$ ). The subscript near the station names indicates the institution providing the data: (a) Puertos del Estado (Spain) and (b) Instituto Hidrográfico (Portugal)

Station Name	Domain	Latitude	Longitude	Period	$R^2$	
					$H_s$	$T_m$
Estaca de Bares <sup>a</sup>	SWE	44.06°N	7.62°W	Jan 02–Dec 09	0.92	0.75
Cabo de Peñas <sup>a</sup>	SWE	43.73°N	6.19°W	Jan 02–Dec 09	0.89	0.71
Villano-Sisargas <sup>a</sup>	SWE	43.49°N	9.21°W	Jan 02–Dec 09	0.90	0.74
Silleiro <sup>a</sup>	PCC	42.12°N	9.40°W	Jan 02–Dec 09	0.91	0.69
Leixões <sup>b</sup>	PCC	41.18°N	8.70°W	Jan 08–Dec 09	0.91	0.61
Sines <sup>b</sup>	PCC	37.92°N	8.92°W	Jan 08–Dec 09	0.90	0.61
Faro <sup>b</sup>	PCC	36.90°N	7.90°W	Jan 08–Dec 09	0.80	0.20
Cadiz <sup>a</sup>	SWE	36.84°N	6.98°W	Jan 08–Dec 09	0.79	0.31

## Wave Resource Assessment

### *Spatial Distribution*

The North Atlantic weather system is largely governed by the so-called North Atlantic Oscillation, which is characterised by the presence of westerly winds (Fig. 14) and a recurring pattern of weather conditions coupled with the Gulf Stream system, with occasional influence of influx of cold weather from the north (Arctic) or the east (Siberia).

This particular weather system generates swells that build over long fetch distances and travel more than 3000 km before reaching the exposed European coasts. Figure 15 shows the distribution of mean significant wave height, from a Wave-Watch III hindcast averaged over a 10-year period. Wave activity and resources along the European Atlantic Coast were characterised by significant wave height ( $H_s$ ), direction ( $\theta$ ), peak period ( $T_p$ ), and power per metre of wave crest ( $P$ ).

The wave climate of the North Atlantic is one of the most energetic of the planet's oceans, particularly in the northern hemisphere and in its approach to the north-western European coast of Ireland and Scotland (Atan et al. 2016). The mean available wave power flux reaches 70 kW/m near the western coast of Ireland and Scotland and approximately 45 kW/h in Galicia at the north-western tip of the Iberian Peninsula (Fig. 16).

This hindcast gives an overview of the wave climate over the North Atlantic basin, but the exploitation of wave energy requires a finer characterisation of wave resources in coastal areas, in particular near irregular coastlines.

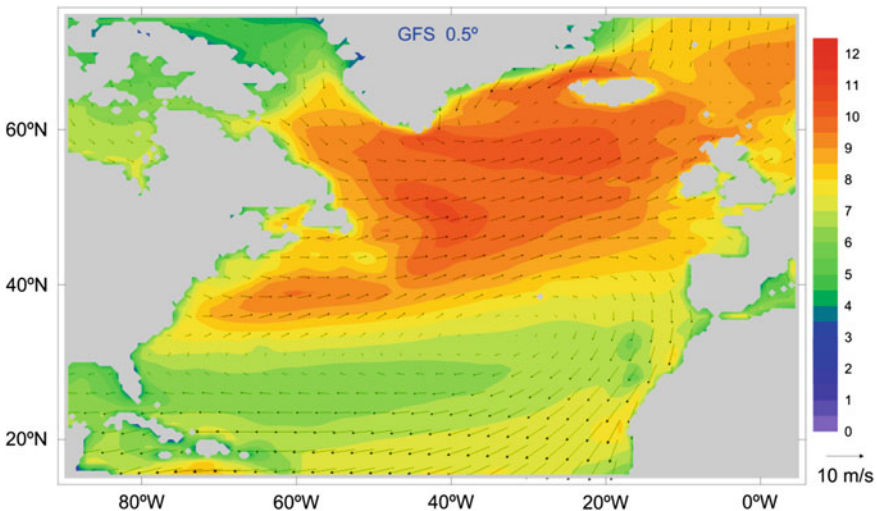


**Fig. 14** Mean wind speed modulus (m/s) and direction over the North Atlantic

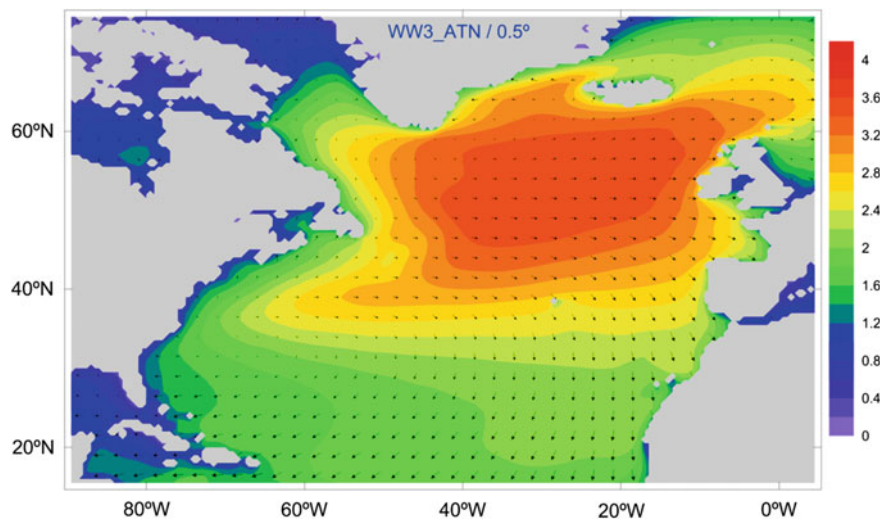


**Fig. 15** Mean significant wave height (m) and direction over the North Atlantic

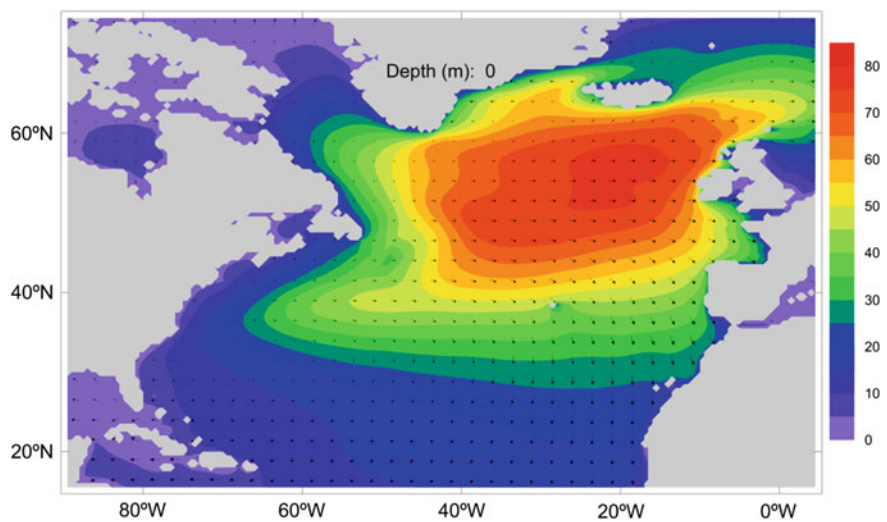


**Fig. 16** Mean wave power density (kW/m) and wave direction over the North Atlantic

Annual and seasonal averages were determined from a 7-year period, 2008–2014. Presented as an atlas of fine-resolution maps, the hindcast shows the variability of the resource at local scale and provides a holistic view of the wave climate along the European Atlantic Coast (Figs. 17 and 18). In addition, the 99 percentile wave height ( $H_{99}$ ) was estimated throughout the modelling period, as an indicator of peak wave activity and therefore potential risk to marine energy installations.

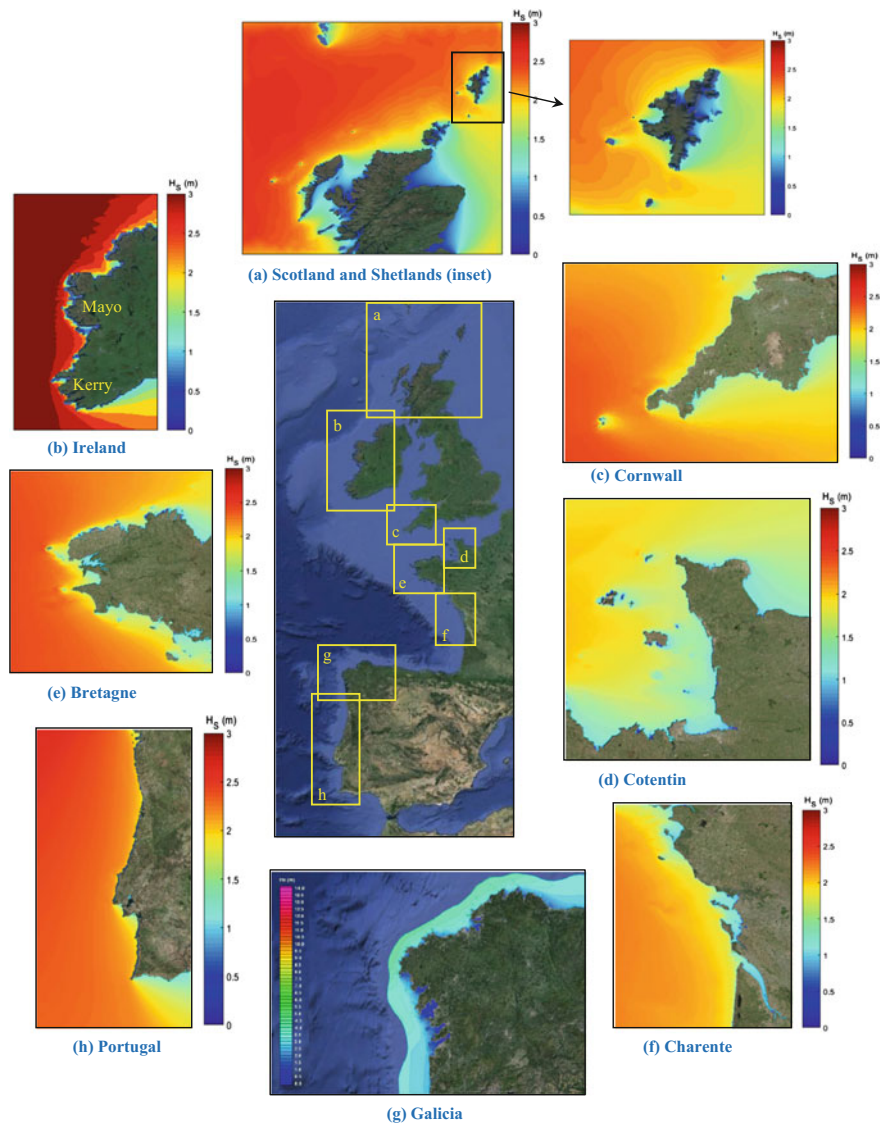


**Fig. 17** Mean significant wave height along the European Atlantic Coast

Around Scotland, waves are higher on the western coast (Fig. 17a). This is mainly due to the predominance of westerly and south-westerly winds combined with longer fetches on the North Atlantic side, which induce strong swells near western Scotland. Nearer to the coasts, the wave height can present a more unequal

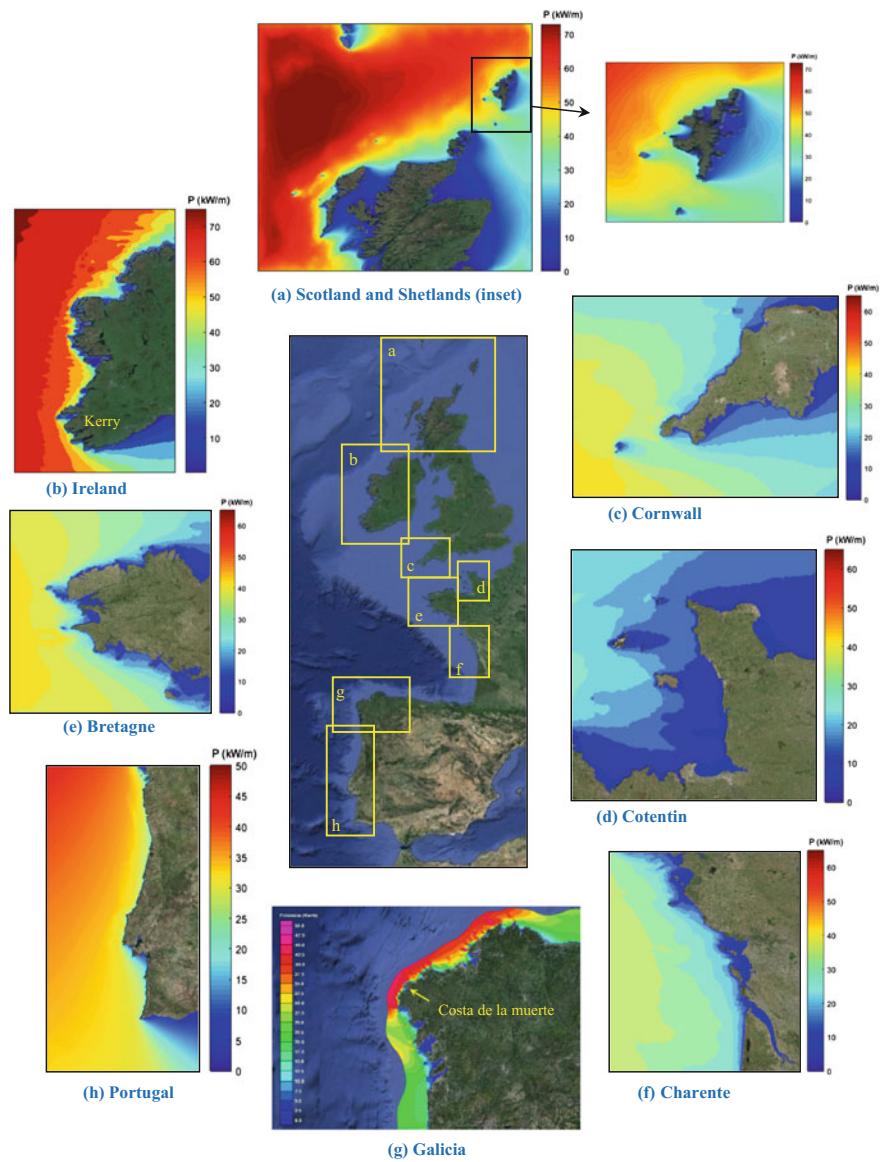


**Fig. 18** Mean wave power density along the European Atlantic Coast

distribution depending on the bathymetry, coastal configuration, and presence of islands, as shown for instance around the Shetland Islands (Fig. 17a). The western coast of Ireland is more frontally exposed to North Atlantic swells and experiences

the highest wave activity in Europe. The mean significant wave height reaches values up to 3 m near its westernmost headlands of counties Mayo and Kerry (Fig. 17b). In comparison, lesser wave activity occurs at lower latitudes where wave heights reach mean values between 2 and 2.5 m near the most exposed headlands of Cornwall, Bretagne, and Galicia, and along the northern to central part of the Portuguese coast. The maps also reveal the variability in wave height distribution over relatively short distances in the presence of islands, as observed for instance around the Shetland Islands, Cotentin, or Bretagne (Fig. 17a, d, and e respectively). Although these local variations in wave height may appear small, they can have a more significant impact on available wave power that is proportional to the square of the significant wave height. The implication of these wave pattern irregularities on the wave power is examined in power density maps for the same areas (Fig. 18). The power density  $P$  is calculated from the significant wave height  $H_S$  and the wave energy period  $T_e$  by:

$$P = \frac{\rho g^2}{64\pi} H_S^2 T_e \quad (2)$$

where  $\rho$  and  $g$  represent the seawater density and gravity acceleration, respectively. This simplified expression uses deep-water approximation (see Nielsen 2009), which fits well most of the modelled domain and all of the locations considered hereafter.

Near the coast, the wave power density tends to concentrate near unsheltered headlands such as the northern tip of the Shetland Islands (Fig. 18a), the westernmost headlands of Kerry County (Fig. 18b), or at Costa de la Muerte in Galicia (Fig. 18g). The fine grid resolution along Galicia shows that the wave power density can vary substantially over short distances (few 10 s of kilometres) near irregular shores. It can be observed that the mean wave power distribution depends on latitude, but probably more significantly on exposure to open waters. As evidence, the highest wave power in European coastal waters was found off the western coasts of Ireland and was estimated to be between 50 and 65 kW/m, except within sheltered bay areas (Fig. 18b).

A comparison of wave characteristics and resources was undertaken at 12 locations distributed over a fair geographical spread along the coast, from the Shetland Islands in the north to the southernmost Portuguese headland of Cabo de São Vicente (Fig. 19 and Table 4). Most of these locations were selected to coincide with the proximity of existing or potential test or energy sites.

The mean values of  $H_S$ ,  $H_{99}$ ,  $T_p$ , and  $P$  were estimated at each location. The depth and exposure to Atlantic swells were variable. The deepest locations were at Kerry, Pontevedra, Belmullet, and Nazaré because of their proximity to the continental shelf slope or to a canyon (Nazaré). Table 4 corroborates the previous observations that wave activity is related to latitude and exposure. The 99 percentile of wave height,  $H_{99}$ , is approximately 2.5 to 3 times higher than  $H_S$ , but these are

**Fig. 19** Selected locations for wave resource variability study



annual averages. Direct observations suggest that this ratio may be dependent on interannual or seasonal variability, in particular with a distinct split between winter and summer months.

### *Seasonal and Interannual Variability*

The seasonal variability is determined for each simulated year by separating and analysing the hindcast data into four seasons: winter (December of previous year to February of current year), spring (March to May), summer (June to August), and

**Table 4** Wave annual statistics

Location	Latitude	Longitude	D (m)	H <sub>S</sub> (m)	H <sub>99</sub> (m)	T <sub>P</sub> (s)	P (kW/m)
Shetlands	60.56°N	1.58°W	78	2.50	7.48	10.8	40.12
Orkneys	58.98°N	3.40°W	54	2.15	5.93	10.5	28.70
Hebrides	58.37°N	6.67°W	30	2.48	6.40	11.1	39.11
Belmullet	54.28°N	10.28°W	89	3.09	7.80	10.6	61.88
Kerry	51.20°N	10.60°W	155	3.13	8.04	10.6	64.52
Cotentin	49.75°N	1.92°W	53	1.20	3.50	6.0	5.33
Bretagne	48.03°N	4.91°W	46	2.20	5.88	10.0	34.12
Landes	44.03°N	1.44°W	38	1.74	5.06	10.5	21.89
Estaca de Bares	44.06°N	7.62°W	46	1.80	5.43	8.7	34.34
Pontevedra	42.12°N	9.40°W	105	1.54	5.96	8.3	29.54
Nazaré	39.59°N	9.12°W	88	1.92	5.32	10.6	24.1
SãoVincente	37.01°N	8.99°W	61	1.90	5.34	10.6	23.1

autumn (September to November). The seasonal average is simply obtained by taking the average of the relevant seasonal values over the period of simulation.

The seasonal variability shows a clear predominance of wave activity during the winter months (Table 5). The difference between summer and winter months appears to be slightly more pronounced in the upper latitudes. A comparison between the different locations, for instance Kerry and Cotentin, highlights the influence of exposure to Atlantic waters on wave resource, but there is no evidence that this exposure could affect the seasonal variability by reducing or enhancing the difference of activity between winter and summer months.

Depending on the weather system, the wave climate has not only a seasonal variability but also an interannual and geographical variability. Figure 20 compares the interannual and seasonal variations of  $H_S$ ,  $H_{99}$ , and  $P$  from 2008 to 2014 at three different locations: the Shetlands, Belmullet, and Bretagne. The wave power density clearly shows the consistent seasonal contrast between summer and winter at all locations. The interannual wave activity during spring and autumn months is more variable. For instance, during autumn 2014,  $H_{99}$  is high in comparison with  $H_S$  for equivalent periods, in particular during winter. This is the signature of peak wave activity over short periods of time.

The geographical difference in wave activity is highlighted by the winter interannual variability. In Bretagne, the highest wave activity is noted during winters 2013 and 2014. In comparison, it is significantly lower during winters 2011 and 2012. Conversely, at the uppermost latitude of the Shetlands, the highest wave activity was noted during winters 2011 and 2012, and it diminished during winters 2013 and 2014. Finally, the interannual and seasonal wave resource estimates at Belmullet appear to be more consistent throughout the period studied, exhibiting a marked lower activity during summer.

Table 5 Wave seasonal statistics

Locations	Hs (m)				H99 (m)				Tp (s)			P (kW/m)					
	Sp	Su	Au	Wi	Sp	Su	Au	Wi	Sp	Su	Wi	Sp	Su	Au	Wi	Au	Wi
Shetlands	2.55	1.39	2.51	3.55	5.46	3.88	6.95	8.88	10.9	9.0	11.1	12.3	36.2	9.6	37.0	78.3	78.3
Orkneys	2.26	1.09	2.24	3.04	4.59	3.23	5.76	6.72	10.7	8.8	10.7	11.9	27.3	5.9	27.7	54.4	54.4
Hebrides	2.65	1.34	2.47	3.47	5.14	3.18	6.29	7.57	11.2	8.9	11.2	12.9	39.2	7.9	34.8	75.2	75.2
Belmullet	2.87	2.09	3.35	4.07	6.84	4.72	7.63	8.78	10.5	8.9	11.0	12.1	49.9	20.7	66.9	111.3	111.3
Kerry	2.92	2.11	3.33	4.22	7.33	4.75	7.90	9.15	10.4	9.0	11.0	12.1	51.7	20.8	68.2	121.6	121.6
Cotentin	1.06	0.97	1.22	1.45	2.97	2.65	3.46	3.52	6.0	5.4	6.0	7.1	4.2	2.9	5.6	8.1	8.1
Bretagne	1.99	1.62	2.28	3.04	5.19	3.76	5.73	6.4	10.1	8.5	10.5	12.0	25.4	12.7	37.0	64.1	64.1
Landes	1.63	1.25	1.74	2.40	4.61	2.86	4.71	5.53	10.7	9.0	11.1	12.5	18.6	7.9	23.4	43.6	43.6
Nazaré	2.22	1.43	1.58	2.47	5.41	3.15	4.31	6.28	11.5	9.0	9.7	12.0	31.0	9.5	14.1	42.1	42.1
São Vicente	2.20	1.41	1.54	2.46	5.63	2.95	4.00	6.12	11.7	8.9	9.7	12.1	30.6	8.4	12.6	41.2	41.2

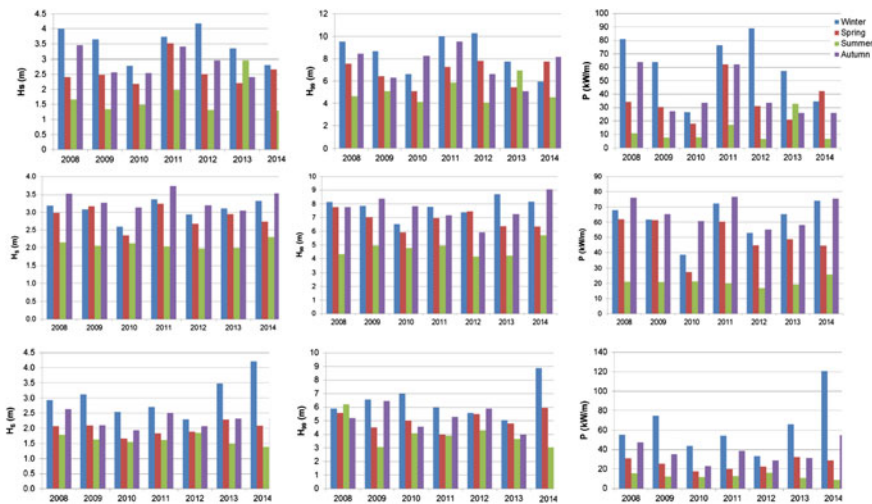


**Fig. 20** Interannual variations of  $H_S$  (first column graphs),  $H_{99}$  (second column), and  $P$  (third column) at Shetland (*top row*), Belmullet (*middle row*), and Bretagne (*bottom row*)

No clear interannual trend can be derived from these estimates. The seasonal variability and differences between the selected locations suggest that the local wave climate is sensitive to mesoscale wind variations ( $\sim 1000$  km) over relatively short periods of time.

## Summary and Discussion

The wave resources along the European Atlantic Coast are characterised using a 7-year hindcast of high-resolution spectral wave models. The modelling domains cover almost the entire European coast from the Shetland Islands in the north to the Portuguese Algarve region in the south, except for Asturias and Cantabria on the northern coast of Spain. The extent and resolution of the models can provide detailed maps of the resource for energy site developers, regulators, and/or potential users and at the same time provide a holistic description of the resource in Europe.

The high-resolution maps show that in coastal areas the wave power can vary significantly over short distances, in particular in the presence of irregular coastlines such as in Galicia, Bretagne, and Ireland, or in the vicinity of islands and archipelagos such as those in Scotland, Cotentin, or Charente. The resource can therefore only be accurately estimated using a fine-resolution grid. Tuomi et al. (2014) showed that inappropriate grid resolution can result in insufficient attenuation of waves in archipelagos and therefore in overestimating the resource. Most spectral wave models can now operate on unstructured meshes, which should be used around complex coastlines.

The wave characteristics and power density were compared at various locations selected near sites of potential interest and fairly distributed along the coastline. The comparisons showed that the wave resource depends essentially on the latitude, but perhaps more importantly on the exposure to Atlantic open waters. Located between 51°N and 55°N and frontally exposed to the North Atlantic, western Ireland has the highest wave energy resource in Europe. The annual average power density at Belmullet (north-west) and Kerry (south-west) has been estimated to be between 60 and 65 kW/m. At these locations, the wave height 99 percentile, which can be used as an indicator of peak wave activity and therefore of potential risk to installations and maintenance operations, can reach 8.5 to 9 metres during the winter months. Annual averaged peak wave periods are estimated to be between 10 and 11 s at most of the selected locations.

The seasonal variability shows a clear and consistent difference between summer (lowest wave activity) and winter (highest wave activity) at all locations. However, no clear trend emerges in the interannual variability. From the investigated locations, the most consistent interannual wave activity was found at Belmullet.

This study provides a detailed description of wave resources along the European Atlantic Coast that investigates both their spatial distribution and temporal variability using hindcast modelling. However, the energy yield of a marine energy site does not only depend on the availability of the resource. Other factors that may influence energy yield include the array layout that can optimise or reduce the resource at a local level, the morphology of the seabed that may change, for instance with accretion or erosion of sediments in sandy areas, or simply affect the local wave patterns by inducing wave breaking, refraction and shoaling, or the local hydrodynamic conditions related, for instance, to tidal currents and water levels.

In addition, wave resources are uncertain because of their inherent unpredictability over the medium to long term, which itself depends on meteorological unpredictability and long-term uncertainties caused by climate change. Statistics from hindcast modelling probably provide the closest evaluation of the resource, which need to be regularly re-evaluated to adjust for longer term changes.

**Acknowledgements** This work was funded by the European Regional Development Fund under the EnergyMare project of the Atlantic Area Programme.

The authors are grateful to INCAT (Ingeniería Civil de Atlántico) for post-processing the model output data and for producing maps of wave height and wave power along the Galician coast, and to Thibault Coulombier and Camille Letretel for their help in providing additional data related to the French coast.

## References

- ABP MER. (2008). Atlas of UK marine renewable energy resources: Atlas pages. A strategic environmental assessment report, Department for Business Enterprise and Regulatory Reform.
- Atan, R., Goggins, J., Hartnett, M., Agostinho, P., & Nash, S. (2016). Assessment of wave characteristics and resource variability at a 1/4-scale wave energy site in Galway Bay using waverider and high frequency radar (CODAR) data. *Ocean Engineering*, 117, 272–291.

- Atan, R., Goggins, J., & Nash, S. (2015). A preliminary assessment of the wave characteristics at the Atlantic Marine Energy Test Site (AMETS) using SWAN. In *Proceedings of the 11th European Wave and Tidal Energy Conference*, Nantes, France.
- Barstow, S., Mollison, D., & Cruz, J. (2008). The wave energy resource. In Cruz, J. (Ed.), *Ocean wave energy* (pp. 40). Springer.
- Barstow, S., Mørk, G., Lønseth, L., & Mathisen J. P. (2009). WorldWaves wave energy resource assessments for the deep ocean to the coast. In *Proceedings of the 8th European Wave and Tidal Energy Conference*, Uppsala, Sweden (pp. 149–159).
- Becker, J. J., Sandwell, D. T., Smith, W. H. F., Braud, J., Binder, B., Depner, J., et al. (2009). Global bathymetry and elevation data at 30 arc seconds resolution: SRTM30\_PLUS. *Marine Geodesy*, 32(4), 355–371.
- Bertotti, L., & Cavaleri, L. (2012). Modelling waves at Orkney coastal locations. *Journal of Marine Systems*, 96–97, 116–121.
- Booij, N., & Holthuijsen, L. H. (1987). Propagation of ocean waves in discrete spectral wave models. *Journal of Computational Physics*, 68(2), 307–326.
- Booij, N., Ris, R. C., & Holthuijsen, L. H. (1999). A third generation model for coastal regions. Part I: model description and validation. *Journal of Geophysical Research*, 104(C4), 7649–7666.
- Cavaleri, L., & Malanotte-Rizzoli, P. (1981). Wind wave prediction in shallow water. Theory and applications. *Journal of Geophysical Research*, 86C11, 10961–10973.
- DHI. (2007). *MIKE21 SW—Spectral waves FM module User guide*. Denmark: Scientific Document, Danish Hydraulic Institute.
- Dietrich, J. C., Zijlma, M., Allier, P. E., Holthuijsen, L. H., Booij, N., Meixner, J. D., et al. (2013). Limiters for spectral propagation velocities in SWAN. *Ocean Modelling*, 70, 85–102.
- European Commission. (2015). Renewable energy progress report, Report from the commission to the European parliament, the council, the European economic and social committee and the committee of the regions, SWD (2015), p. 117.
- Gleizon, P., Campuzano F. J., Carracedo García, P., Gomez B., & Martinez, A. (2015). Wave energy mapping along the European Atlantic coast. In *Proceedings of the 11th European Wave and Tidal Energy Conference*, Nantes, France.
- Gleizon, P., & Murray, A. (2014). Modelling wave energy in archipelagos—Case of northern Scotland. In *Proceedings of the 2nd Environmental Interactions of Marine Renewable Energy Technologies*, Stornoway, United Kingdom.
- Gleizon, P., & Woolf, D. (2013). Wave energy assessment in Scotland. In *Proceedings of the 10th European Wave and Tidal Energy Conference*, Aalborg, Denmark.
- Guedes Soares, C., Weisse, R., Carretero, J. C., & Alvarez, E. (2002). A 40 years hindcast of wind, sea level and waves in European waters. In *Proceedings of the 21st International Conference on Offshore Mechanics and Arctic Engineering (OMAE 2002)*, Oslo, Norway.
- Guillou, N. (2015). Evaluation of wave energy potential in the Sea of Iroise with two spectral models. *Ocean Engineering*, 106, 141–151.
- Guillou, N., & Chapalain, G. (2015). Numerical modelling of nearshore wave energy resource in the Sea of Iroise. *Renewable Energy*, 83, 942–953.
- Hasselmann, K. (1962). On the nonlinear energy transfer in a gravity-wave spectrum—Part I. General Theory. *Journal of Fluid Mechanics*, 12, 481–500.
- Hasselmann, K., Barnett, T. P., Bouws, E., Carlson, H., Cartwright D. E., Enke, K., et al. (1973). Measurements of wind-wave growth and swell decay during the Joint North Sea Wave Project (JONSWAP). *Deutschen Hydrographischen Zeitschrift, Suppl. A*(8) n° 12, pp. 95.
- Hersbach, H., & Janssen, P. A. E. M. (1999). Improvement of the short-fetch behavior in the wave ocean model (WAM). *Journal of Atmospheric and Oceanic Technology*, 16, 884–892.
- Iglesias, G., & Carballo, R. (2009). Wave energy potential along the Death Coast (Spain). *Energy*, 34, 1963–1975.
- Iglesias, G., & Carballo, R. (2010a). Offshore and inshore wave energy assessment: Asturias (N Spain). *Energy*, 35, 1964–1972.
- Iglesias, G., & Carballo, R. (2010b). Wave energy and nearshore hot spots: The case of the SE Bay of Biscay. *Renewable Energy*, 35, 2490–2500.

- Iglesias, G., & Carballo, R. (2010c). Wave energy resource in the Estaca de Bares area (Spain). *Renewable Energy*, 35, 1574–1594.
- Iglesias, G., Lopez, M., Carballo, R., Castro, A., Fraguera, J. A., & Frigaard, P. (2009). Wave energy potential in Galicia (NW Spain). *Renewable Energy*, 34, 2323–2333.
- Komen, G. J., Hasselmann, S., & Hasselmann, K. (1984). On the existence of a fully developed wind-sea spectrum. *Journal of Physical Oceanography*, 14, 1271–1285.
- Leonard, B. P. (1979). A stable and accurate convective modelling procedure based on quadratic upstream interpolation. *Computer Methods in Applied Mechanics and Engineering*, 18, 17–74.
- Leonard, B. P. (1991). The ULTIMATE conservative difference scheme applied to unsteady one-dimensional advection. *Computer Methods in Applied Mechanics and Engineering*, 88, 59–98.
- Lopez, I., Andreu, J., Ceballos, S., Martínez de Alegría, I., & Kortabarria, I. (2013). Review of wave energy technologies and the necessary power-equipment. *Renewable and Sustainable Energy Reviews*, 27, 413–434.
- May, V. J., Hansom, J. D. (2003). Coastal geomorphology of Great Britain, Geological Conservation Review Series (Vol. 28, pp. 754). ISBN 1 86107 484 0.
- NCEP/NWS/NOAA/U.S. Department of Commerce. (2000). NCEP FNL Operational Model Global Tropospheric Analyses, continuing from July 1999, Research Data Archive at the National Center for Atmospheric Research, Computational and Information Systems Laboratory, Boulder, Colorado. Retrieved February 11, 2015, from <http://dx.doi.org/10.5065/D6M043C6>.
- Nielsen, P. (2009). *Coastal and Estuarine processes, advanced series on ocean engineering* (Vol. 29). World Scientific.
- NREAP (National Renewable Energy Action Plan). (2010). <http://ec.europa.eu/energy/en/topics/renewable-energy/national-action-plans>.
- Piollé, J. F., Croizé-Fillon, D. (2012). Operation of CERSAT data centre. Ifremer report 13/2 213 213.
- Pontes, M. T. (1998). Assessing the European wave energy resource. *Journal of Offshore Mechanics and Arctic Engineering*, 120(4), 226–231.
- Pontes, M. T., Athanassoulis, G. A., Barstow, S., Bertotti, L., Cavaleri, L., Holmes, B., et al. (1998). The European wave energy resource. In *Proceedings of the 3rd European Wave Energy Conference*, Patras, Greece.
- Robertson, B. (2017). Wave energy assessments: quantifying the resource and understanding the uncertainty. In Z. Yang & A. Copping (Ed.), *Marine renewable energy: Resource characterization, practical energy harvest and effects on physical systems*. Springer.
- Robertson, B., Hiles, C., & Buckham, B. (2014). Characterizing the near shore wave energy resource on the west coast of Vancouver Island. *Canada, Renewable Energy*, 71, 665–678.
- Robertson, B., Hiles, C., Luczko, E., & Buckham, B. (2016). Quantifying wave power and wave energy converter array production potential. *International Journal of Marine Energy*, 14, 143–160.
- Roland, A. (2009) *Development of WWM II: Spectral wave modelling on unstructured meshes*, Ph. D. thesis, Technische University at Darmstadt, Institute of Hydraulic and Water Resources Engineering.
- Stelling, G. S., & Leendertse J. J. (1992). Approximation of convective processes by cyclic AOI methods. In *Proceedings of 2nd International Conference on Estuarine and Coastal Modelling*, ASCE Tampa, Florida (pp. 771–782).
- Tolman, H. L. (1990). A third-generation model for wind waves on slowly varying, unsteady, and inhomogeneous depths and currents. *Journal of Physical Oceanography*, 21, 782–797.
- Tolman, H. L. (2002). Alleviating the garden sprinkler effect in wind wave models. *Ocean Modelling*, 4, 269–289.
- Tuomi, L., Pettersson, H., Fortelius, C., Tikka, K., & Björkqvist, Kahma K. K. (2014). Wave modelling in archipelagos. *Coastal Engineering*, 83, 205–220.

- Van der Westhuysen, A. J., Zijlema, M., & Battjes, J. A. (2007). Nonlinear saturation-based whitecapping dissipation in SWAN for deep and shallow water. *Coastal Engineering*, 54, 151–170.
- Venugopal, V., & Nimaladinne, R. (2015). Wave resource assessment for Scottish waters using a large scale North Atlantic spectral wave model. *Renewable Energy*, 76, 503–525.
- WAMDI group (1988) The WAM model—a third generation wave prediction model, *Journal of Physical Oceanography*, 18, 1775–1810.
- WISE Group. (2007). Wave modeling—The state of the art. *Progress in Oceanography*, 75, 603–674.
- Yang, Z., & Wang T. (2015). Modelling wave resource characterization using an unstructured grid coastal ocean model. In *Proceedings of the 11th European Wave and Tidal Energy Conference 2015*, Nantes, France.
- Zijlema, M. (2010). Computation of wind-wave spectra in coastal waters with SWAN on unstructured grids. *Coastal Engineering*, 57, 267–277.

Marine Renewable Energy

Resource Characterization and Physical Effects

Yang, Z.; Coppng, A. (Eds.)

2017, XIV, 387 p. 144 illus., 135 illus. in color.,

Hardcover

ISBN: 978-3-319-53534-0